Adsorption Kinetics of Some Polyethylene Glycol Octylphenyl Ethers Studied by the Fast Formed Drop Technique

Tommy Horozov[1,2] and Luben Arnaudov

Laboratory of Thermodynamics and Physico-Chemical Hydrodynamics, Sofia University, Faculty of Chemistry,
1 James Bourchier Ave., Sofia 1126, Bulgaria

The adsorption kinetics of Triton X-100 and Triton X-405 at solution/air and solution/hexane interfaces is studied by the recently developed fast formed drop technique. The dynamic interfacial tension of Triton X-100 and Triton X-405 solutions against hexane has been measured without preequilibration of the water and oil phases. It is found that the dynamic interfacial tension of Triton X-100 solutions passes through a minimum. This strange behavior is attributed to partial solubility of the surfactant in hexane. Such minima of the dynamic interfacial tension of Triton X-405 solutions have not been observed, which correlates well with the solubilities of both surfactants in hexane reported in the literature.

The dynamic surface tension of solutions of both surfactants and the dynamic interfacial tension of Triton X-405 solutions are interpreted by the Ward and Tordai model for diffusion controlled adsorption. It is shown that proper interpretation of the experimental data depends on the type of isotherm used. More consistent results are obtained when the Temkin isotherm is used instead of the Langmuir isotherm.

The results obtained with Triton X-100 at the solution/air interface confirm that the adsorption of this surfactant occurs under diffusion control. The adsorption of Triton X-405 at solution/air and at solution/hexane interfaces seems to occur under diffusion control at short periods of time, but under mixed (diffusion–kinetic) control at long periods of time. A hypothesis is drawn to explain this phenomenon by changes in the shape of the large hydrophilic heads of Triton X-405 molecules.   © 2000 Academic Press

Key Words: adsorption kinetics; fast formed drop technique; polyethylene glycol octylphenyl ethers; Triton X-100; Triton X-405.

INTRODUCTION

Polyethylene glycol octylphenyl ethers, $C_{14}H_{21}O(C_2H_4O)_nH$, are biphilic compounds with different numbers of ethoxy groups, n, incorporated in their molecules. A gradual increase of n (say from 1 to several tens) leads to a gradual change in their properties. They are typical nonionic surfactants widely used commer-

cially as detergents, emulsifiers, wetting agents, etc. (1–3). The adsorption from their solutions at water/air and water/oil interfaces was intensively studied during the last decade (4–13). A lot of these studies deal with the adsorption kinetics of Triton X-100 ($n = 10$) and Triton X-405 ($n = 40$) at a water/air interface (4, 6–11). It is found that the adsorption of these surfactants occurs under diffusion control. However, there are some peculiarities of their adsorption properties, which are still not very clear and some contradictions among published data exist. For instance, it is known that the Langmuir adsorption isotherm is operative for many nonionic surfactants (14). It can also be applied in the case of Triton X-100 and Triton X-405. However, it is found that when the Langmuir isotherm is used, the results obtained by dynamic experiments cannot be described in a satisfactory way, while by the use of the Temkin isotherm they can (4, 7, 11). Lin *et al.* (6) found that the Frumkin isotherm describes equilibrium surface tension data better than the Langmuir isotherm at low concentrations of Triton X-100. They have obtained reasonable values for the diffusivity D of this surfactant ($D = 2.6 \times 10^{-6}$ cm^2/s) from dynamic surface tension (DST) data by means of the former isotherm. Fainerman *et al.* (9) have studied the adsorption kinetics of six polyethylene glycol octylphenyl ethers with n ranging from 4.5 to 40 (including Triton X-100 and Triton X-405) by the maximum bubble pressure method. The equilibrium adsorptions Γ_e of the surfactants studied have been calculated from the kinetic data at long periods of time by using diffusivity values in the range from 0.7×10^{-6} to 0.95×10^{-6} cm^2/s, depending on the molecular weight of the surfactant. The Γ_e values obtained have been in good agreement with those calculated by means of the Langmuir isotherm. The Langmuir model of adsorption also gave consistent results in the case of some mixtures of the surfactants studied (9). Some peculiarities with respect to the adsorption kinetics at short and long periods of time have been pointed out in Ref. (8). The authors have studied the dynamic surface tension of Triton X-100 and Triton X-405 aqueous solutions by the maximum bubble pressure and the inclined plate methods in the time range from 0.001 s up to 10 s. They have found that the fast decrease of the dynamic surface tension at short periods of time cannot be described in a satisfactory way by means of the diffusivity values equal to 0.88×10^{-6} cm^2/s and 0.7×10^{-6} cm^2/s

[1] Present address: CHIMATECH Corp., Surfactants Division, 14 Iskarsko Shosse Blvd., Sofia 1592, Bulgaria.

[2] To whom correspondence should be addressed. E-mail: chimatech@ mbox.cit.bg.

146

for Triton X-100 and Triton X-405, respectively, calculated from the data at long periods of time. They have concluded that adsorption kinetics at short periods of time is much faster than that at long periods of time. In order to explain this effect, they have proposed a theoretical model based on a hypothesis for the adsorption of polyethylene glycol chains (the hydrophilic heads of the surfactants) at the solution/air interface at small and medium values of the surface pressure (i.e., at short and medium periods of time) and the partial or total submergence of the hydrophilic chains in the water phase at large surface pressures (i.e., at long periods of time). This model has been further developed and supported with kinetic studies performed over a wide temperature range (10). The adsorption kinetics of the surfactants considered at solution/oil interfaces is less studied (4, 5, 12). Some of the published results contradict the findings at the solution/air interface described above. Liggieri *et al.* have studied the dynamic interfacial tension (DIT) of Triton X-100 solutions against hexane by the so-called expanded drop technique in the time range from 0.1 s up to 400 s (12). The results have been interpreted assuming diffusion controlled adsorption by use of the Freundlich isotherm. The latter is found to be operative for the system studied (13). The diffusivity calculated in Ref. (12) from the data at short periods of time is equal to about 1.4×10^{-6} cm²/s, while that calculated by means of the long time approximation is much greater and equal to 9.2×10^{-6} cm²/s. These results suggest that the adsorption kinetics at long periods of time is faster than that at short periods of time. This contradicts the findings of Fainerman *et al.* at the solution/air interface (8).

In our previous work, we have developed the so-called fast formed drop (FFD) technique (15). There, we have demonstrated the applicability of this technique for well-reproducible measurements of the dynamic surface and interfacial tension of Triton X-100 and Triton X-405 solutions at constant interfacial area in the time domain from 50 ms up to several minutes. The results obtained were compared with those measured by the static drop weight method but were not quantitatively interpreted. The present work aims to interpret kinetic data obtained at solution/air and solution/hexane interfaces and (if possible) to clarify some of the contradictions pointed out above. For that purpose, some additional measurements of the dynamic surface and interfacial tension of Triton X-100 and Triton X-405 solutions are made. The experimental data are interpreted by means of the Langmuir isotherm and by the Temkin isotherm, and the results obtained are compared.

MATERIALS

The surfactants used in the present study were Triton X-100 and Triton X-405, both purchased from Serva and used without further purification. The DIT measurements were performed with *n*-hexane (Aldrich, 99% purity). The water phase was not preliminarily saturated with oil in these experiments and vice versa. Deaerated water, prepared as described previously (15), was used in all experiments.

METHODS

The experimental setup and the experimental procedure of the FFD technique were described in detail in our previous work (15). Here, we will review briefly the main points. A sketch of the experimental set-up is shown in Fig. 1. One end of a glass capillary with an outer radius $R_c = 0.0659$ cm is connected to a reservoir of surfactant solution and to a precise pressure transducer. A stopcock is mounted in the pipeline not far from the capillary. When the stopcock is closed, the transducer can measure the pressure inside the compartment with the capillary. The output signal of the transducer is amplified and by means of an analog-to-digital converter (ADC) is stored in a file on a PC. The time t is measured by the PC's clock and is recorded in a file as well. The capillary is mounted inside the left branch of a U-shaped vessel partially filled with solution. When the stopcock is open, the solution flows from the reservoir through the capillary as a jet (Fig. 1a). After several seconds, the stopcock is closed, the flow stops, and the jet breaks off very fast. This moment is taken as the beginning of the adsorption process ($t = 0$). The small drop remaining at the capillary tip after stopping the flow (Fig. 1b) is observed by a long focus microscope, while the pressure inside the drop is measured by the transducer, and its output signal is recorded. The height H of the drop and the depth of immersion Δz of the capillary in the oil (when the DIT is studied) are measured by the microscope (Fig. 1b). The output voltage U_0 of the pressure transducer corresponding to a flat solution/air surface at the capillary tip is determined before measurements are made as described previously (15). The DST and the DIT are calculated by the equation

$$P_c(t) = \frac{2\sigma(t)}{R} = \frac{\partial P}{\partial U}[U(t) - U_0] - \Delta\rho g \Delta z, \qquad [1]$$

where $P_c(t)$, $U(t)$, and $\sigma(t)$ are the capillary pressure, the output voltage of the transducer, and the dynamic surface (interfacial) tension at time t, respectively; $R = (H^2 + R_c^2)/(2H)$ is the radius of the spherical drop attached at the capillary tip (Fig. 1b); $\Delta\rho$ is the difference between the densities of the drop liquid and the surrounding fluid, g is the acceleration of gravity; and R_c is the outer radius of the capillary tip. The first term on the right-hand side of Eq. [1] is the pressure measured by the transducer, while the second term is the hydrostatic pressure due to immersion of the capillary in the oil phase. The constant $\partial P/\partial U = 450$ dyn/cm² per volt was preliminarily determined by experiments with pure water (15).

Some measurements of the DST of Triton solutions have been made by the static drop weight method as described in our previous work (15).

All experiments were performed at room temperature (24°C).

RESULTS

The DST of Triton X-100 and Triton X-405 solutions are plotted in Figs. 2 and 3, respectively. The data obtained by the FFD
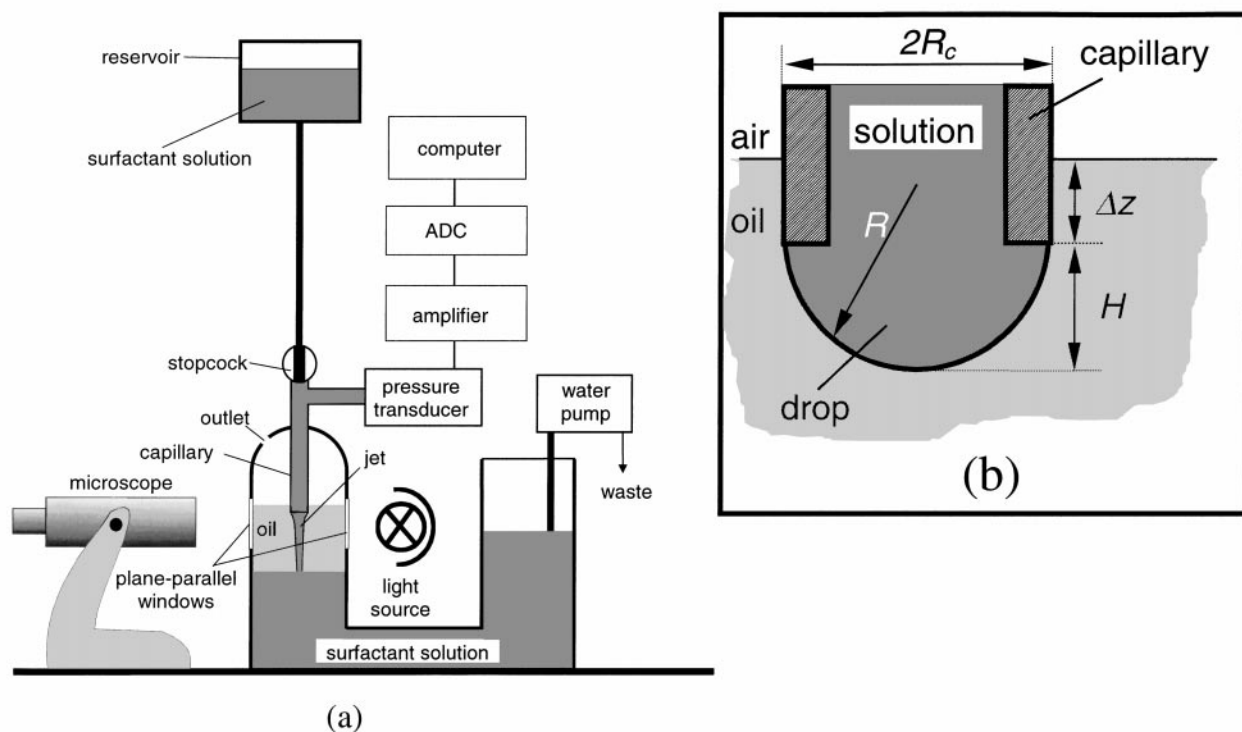
FIG. 1. Sketch of the experimental setup (a) and close-up of the capillary tip (b).

technique (solid figures) are collected from at least four runs at each surfactant concentration and confirm the good reproducibility of the measurements. The data measured by the static drop weight method (empty figures) are also shown in Figs. 2 and 3 for comparison. The discrepancies observed between DST at short periods of time can be attributed to the greater initial adsorption of the surfactants in the static drop weight experiments compared to that in the FFD measurements (15).
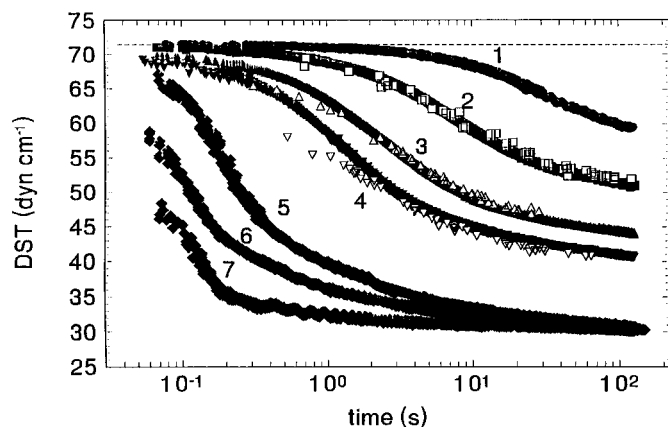
The dynamic interfacial tension of Triton X-100 and Triton X-405 solutions against *n*-hexane are plotted in Figs. 4 and 5, respectively. A well-pronounced minimum in the DIT of the most concentrated Triton X-100 solution (curve 5a in Fig. 4) is seen. In order to check if this behavior is due to surfactant transfer from the solution into the oil phase, we have measured the DIT of the same solution, but after preequilibration with hexane for a certain time. The DIT of the preequilibrated system for 15 h
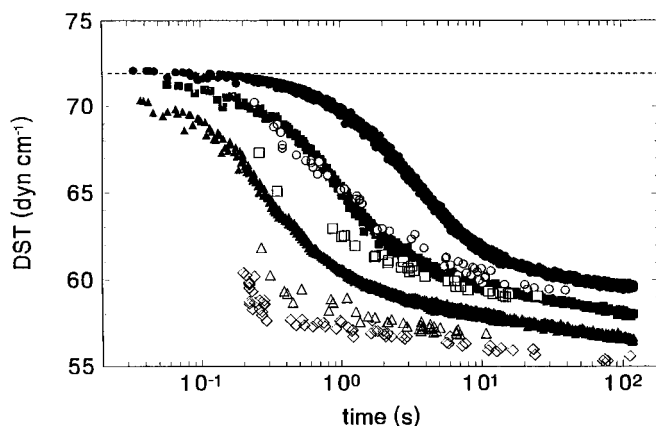

FIG. 2. Dynamic surface tension of Triton X-100 solutions measured by the FFD technique (solid figures) and by the static drop weight method (empty figures) at concentrations ($\times 10^8$ mol cm^{-3}) equal to 1.0 (1); 2.58 (2, $\square$); 5.0 (3, $\triangle$); 7.5 (4, $\triangledown$); 23.25 (5); 31.0 (6); and 62.0 (7). The dashed line shows the lower limit of validity of Eqs. [6] and [7].

FIG. 3. Dynamic surface tension of Triton X-405 solutions measured by the FFD technique (solid figures) and by the static drop weight method (empty figures) at concentrations ($\times 10^8$ mol cm^{-3}) equal to 1.25 ($\bullet$); 1.75 ($\bigcirc$); 2.5 ($\blacksquare$, $\square$); 5.0 ($\blacktriangle$, $\triangle$); and 7.6 ($\diamond$). The dashed line shows the lower limit of validity of Eqs. [6] and [7].
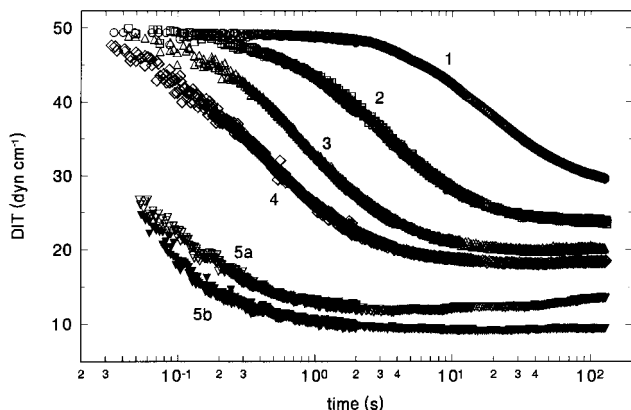
FIG. 4. Dynamic interfacial tension of Triton X-100 solutions against hexane measured by the FFD technique at concentrations ($\times 10^8$ mol cm^{-3}) equal to 1.0 (1); 2.58 (2); 5.0 (3); 7.5 (4); 23.25 (5a, 5b) without preequilibration of oil and water phases (1–5a) and after 15 h of preequilibration of the phases (5b).

is lower, and the minimum is hardly visible (curve 5b in Fig. 4). This is not the case with Triton X-405 solutions, where neither minima nor a significant effect of preequilibration of the phases is observed (see Fig. 5).

DISCUSSION

Theoretical Considerations

The data measured by the FFD technique are obtained at a constant interfacial area. Hence the Ward and Tordai equation for diffusion controlled adsorption (16) can be applied to interpret the results. It reads

$$\Gamma(t) = \Gamma(0) + 2\sqrt{\frac{D}{\pi}} \int_0^{\sqrt{t}} [c_e - c_s(t - \xi)] \, d\sqrt{\xi}. \quad [2]$$
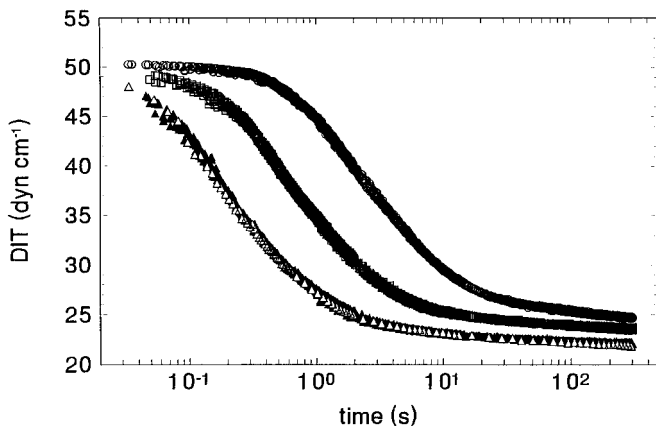

FIG. 5. Dynamic interfacial tension of Triton X-405 solutions against hexane measured by the FFD technique at concentrations ($\times 10^8$ mol cm^{-3}) equal to 1.25 ($\bigcirc$), 2.5 ($\square$), and 5.0 ($\triangle$, $\blacktriangle$) without preequilibration of oil and water phases ($\bigcirc$, $\square$, $\triangle$) and after 15 h of preequilibration of the phases ($\blacktriangle$).

Here $\Gamma(t)$ is the surfactant adsorption at time t, $\Gamma(0)$ is the initial adsorption, D is the diffusivity, c_e is the surfactant concentration in the bulk far from the interface, c_s is the subsurface concentration, and ξ is a dummy variable. The initial adsorption $\Gamma(0)$ is assumed to be equal to zero in the original work of Ward and Tordai (16), but we will keep this term in our considerations. Equation [2] with $\Gamma(0) \neq 0$ is sometimes called the modified Ward and Tordai equation (4, 5). Strictly speaking, Eq. [2] is for the case of diffusion toward a plane interface, whereas in our experiments the interface is curved. However, the diffusion process occurs in a very thin layer, whose thickness is much smaller than the drop radius. That is why Eq. [2] can also be used in our case. In order to avoid integration, approximate solutions of Eq. [2] at long or at short periods of time are usually used for interpretation of the experimental data.

Following the approach of Joos et al. (17, 18), i.e., assuming that $c_s \cong$ const. at long periods of time, Eq. [2] can be easily integrated and a long time approximated solution can be obtained. The solution derived by Joos et al. (17, 18) has been compared with other approximate solutions in Ref. (19), where its reliability for interpretation of the kinetic data at long periods of time is discussed. Taking into account the Gibbs equation

$$\Gamma_e = -\frac{1}{R_g T} \frac{d\sigma_e}{d \ln c_e}, \quad [3]$$

after integration of Eq. [2], we obtain

$$\sigma(t) = \sigma_e + \left(1 - \frac{\Gamma(0)}{\Gamma_e}\right) \frac{R_g T \Gamma_e^2}{2c_e} \sqrt{\frac{\pi}{D}} \frac{1}{\sqrt{t}}. \quad [4]$$

Here σ_e and Γ_e are the equilibrium surface (interfacial) tension and the equilibrium adsorption, respectively; R_g is the gas constant, and T is temperature. Since we kept $\Gamma(0) \neq 0$, our solution (i.e., Eq. [4]) differs from that of Joos et al. (17, 18) by the term $1 - \Gamma(0)/\Gamma_e$. Hence, the slope of the line $\sigma = \sigma(t^{-1/2})$ defined by Eq. [4] depends also on the initial adsorption. A greater $\Gamma(0)$ leads to a smaller slope. The equilibrium surface tension can be obtained from the intercept of the linear plot σ versus $t^{-1/2}$, while the surfactant diffusivity D can be calculated from the slope if Γ_e and $\Gamma(0)$ are known. Disregarding $\Gamma(0)$ in Eq. [4] will lead to some overestimation of D in these calculations. The initial adsorption can be obtained from the data at short periods of time (see below).

At short periods of time, when $c_s \ll c_e$, Eq. [2] reduces to

$$\Gamma(t) = \Gamma(0) + 2c_e\sqrt{\frac{D}{\pi}}\sqrt{t}. \quad [5]$$

Hence, the diffusivity D and the initial adsorption $\Gamma(0)$ can be obtained from the slope and the intercept of the linear plot Γ vs $t^{1/2}$. Surfactant adsorption $\Gamma(t)$ can be calculated from the measured DST values $\sigma(t)$ by means of the adsorption isotherm, if a local equilibrium between the surface and the subsurface at

$t > 0$ is assumed. Very often a linear relationship between Γ and c_s is assumed (the Henry isotherm) for interpretation of the data at short periods of time. This means that the adsorption layer behaves like an ideal two-dimensional gas according to the equation

$$\Delta\sigma = \sigma_0 - \sigma = R_g T \Gamma, \tag{6}$$

where $\Delta\sigma$ is the surface pressure and σ_0 is the surface (interfacial) tension of the pure solvent. The substitution of Eq. [5] (with $\Gamma(0) = 0$) in Eq. [6] yields

$$\Delta\sigma(t) = 2 R_g T c_e \sqrt{\frac{D}{\pi}} \sqrt{t}. \tag{7}$$

Usually, Eq. [7] is used without any analysis of its range of validity. To do such an analysis, let us take the Langmuir isotherm which reads

$$\Gamma = \Gamma_\infty \frac{c/a}{1 + c/a}. \tag{8}$$

Here Γ_∞ is the saturation adsorption, and a is called a Langmuir constant. It is known that the Langmuir isotherm reduces to the linear Henry isotherm under condition $c/a \ll 1$. Thus c/a can be neglected in the denominator of Eq. [8]. To do so, one can assume that $c/a \leq 0.1$. Hence $\Gamma \leq 0.1\,\Gamma_\infty$. After substitution of the latter condition in Eq. [6], we obtain the following criterion for the validity of Eq. [7]:

$$\sigma(t) \geq \sigma_0 - 0.1 R_g T \Gamma_\infty. \tag{9}$$

It is found out that in the particular case of Triton X-100 and Triton X-405, Γ_∞ is equal to 3.3×10^{-10} mol/cm^2 and 1.4×10^{-10} mol/cm^2, respectively (9). Hence, Eq. [7] can be applied if $\sigma(t) \geq \sigma_0 - 0.8$ in the case of Triton X-100 and if $\sigma(t) \geq \sigma_0 - 0.3$ in the case of Triton X-405. The calculated limiting values of the DST are shown in Figs. 2 and 3 (dashed lines). Obviously, Eq. [7] cannot be used for interpretation of our data because the DST of the solutions studied are out of the range of validity of Eqs. [6] and [7] (except the most dilute solutions). That is why Eq. [5] has to be used together with some nonlinear isotherm (e.g., the Langmuir isotherm). Equation [8] coupled with Eq. [3] gives

$$\Gamma = \Gamma_\infty \left[1 - \exp\left(-\frac{\sigma_0 - \sigma}{R_g T \Gamma_\infty} \right) \right] \tag{10}$$

and

$$\sigma_e = \sigma_0 - R_g T \Gamma_\infty \ln\left(1 + \frac{c}{a} \right). \tag{11}$$

The adsorption $\Gamma(t)$ can be calculated from the DST data by Eq. [10]. Then Eq. [5] can be applied at short periods of time.

The constant Γ_∞ can be obtained from the fit of the equilibrium surface tension data versus surfactant concentration by means of Eq. [11]. There is not a commonly accepted type of isotherm for Triton X-100 and Triton X-405, as we pointed out in the introductory section of the present work. In order to check the importance of the type of isotherm for the interpretation of the experimental data, we also used the Temkin isotherm. The latter reads

$$\sigma_e = \sigma_0 - \alpha \Gamma_e^2, \tag{12}$$

where α is a constant. When coupled with Eq. [3], it gives (4)

$$\Gamma_e = \frac{R_g T}{2\alpha} \ln c_e + \frac{k1}{\sqrt{\alpha}} \tag{13}$$

and

$$\sigma_e = \sigma_0 - \left(\frac{R_g T}{2\sqrt{\alpha}} \ln c_e + k_1 \right)^2, \tag{14}$$

where k_1 is another constant. The Temkin isotherm has a disadvantage that it does not predict ideal behavior of the adsorption layer at small surface pressures (see Eq. [6]), as the Langmuir isotherm does. However, the above analysis showed that most of our experimental data are out of the range of ideal behavior of the adsorption layer. Hence, the Temkin isotherm can be used for the interpretation of our data.

Based on the above considerations, we can apply the following consecutive steps for the interpretation of the results: (i) determination of the equilibrium surface (interfacial) tension σ_e and the slope $\partial\sigma/\partial(t^{-1/2})$ according to Eq. [4] at long periods of time; (ii) determination of the constants ($\Gamma_\infty, a, \alpha, k_1$) of the adsorption isotherms from the fits of σ_e versus c_e dependencies by means of Eqs. [11] and [14]; (iii) calculation of $\Gamma(t)$ from the measured DST by using Eqs. [10] and [12] and determination of $\Gamma(0)$ and D according to Eq. [5]; and (iv) calculation of D from the slope $\partial\sigma/\partial(t^{-1/2})$ at long periods of time by using the initial adsorption $\Gamma(0)$ obtained and Γ_e calculated by Eqs. [8] and [13] in the case of the Langmuir or Temkin isotherm, respectively. Finally, the diffusivity values obtained by short and long time approximations can be compared to each other and to the expected value D_{expect}. The latter can be estimated by means of the Stokes-Einstein equation as described elsewhere (20, 21). We obtained $D_{\text{expect}} = 3.5 \times 10^{-6}$ cm^2/s for Triton X-100 (MW = 647, $d_4^{20} = 1.07$ g/cm^3) and $D_{\text{expect}} = 2.4 \times 10^{-6}$ cm^2/s for Triton X-405 (MW = 1967, $d_4^{20} = 1.10$ g/cm^3).

Interpretation of the Results

The DST of the solutions studied measured by the FFD technique and by the static drop weight method are plotted versus $t^{-1/2}$ in Figs. 6 and 7. As expected, the DST of the three most concentrated Triton X-100 solutions tend to the same σ_e value because their concentrations are above the CMC (4, 6). Although
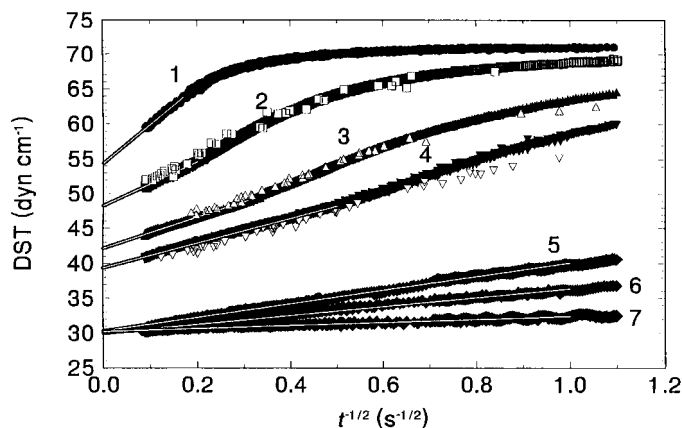
FIG. 6. Dynamic surface tension of Triton X-100 solutions versus $t^{-1/2}$. Notations are the same as in Fig. 2.

FIG. 8. Extrapolated to infinite time DST (circles and boxes) and DIT (triangles) values of Triton X-100 (boxes) and Triton X-405 (circles and triangles) solutions obtained by the FFD technique (solid figures), the static drop weight method ($\bigcirc$, $\square$), the maximum bubble pressure method in Ref. (37) ($\boxtimes$, $\otimes$), and by the Wilhelmy plate method in Ref. (38) ($\triangle$). The lines are the best fits according to Eq. [14] (solid lines) and Eq. [11] (dashed lines).

the DST measured by the static drop weight method is smaller than that measured by the FFD technique at short periods of time, they practically tend to the same value at long periods of time. It is easily seen (especially in Fig. 7) that the slopes $\partial\sigma/\partial(t^{-1/2})$ obtained by the former method are smaller than that obtained by the FFD technique. In view of Eq. [4], the latter fact is in accordance with our previous conclusion for greater initial adsorption in the static drop weight method in comparison to the FFD technique (15). The extrapolated DST values at infinite time (the intercepts) obtained by both methods are plotted as a function of surfactant concentration in Fig. 8, where the data of Fainerman *et al.* (9) obtained by the MBPM are also presented for comparison. Very good agreement is seen in the results, although they have been obtained by different methods.

The equilibrium surface tension values obtained by us are fitted with Eqs. [11] and [14] (see the lines in Fig. 8). The parameters of the best fits are summarized in Table 1. The equilibrium adsorption was calculated by Eqs. [8] or [13], whereas Eqs. [10] and [12] were used for calculation of the surfactant adsorption $\Gamma(t)$ from measured DST data. The plots of Γ/Γ_e
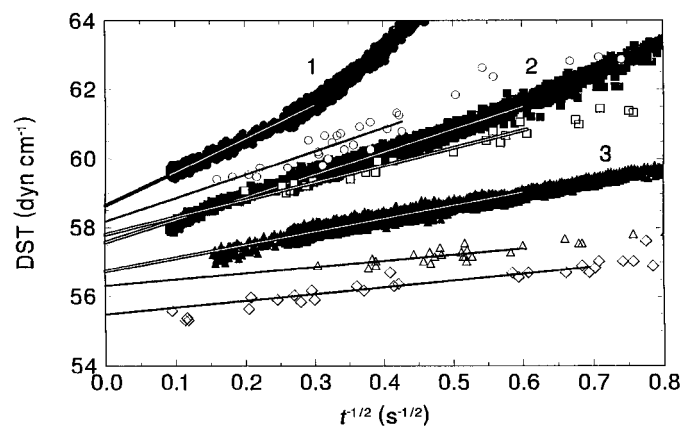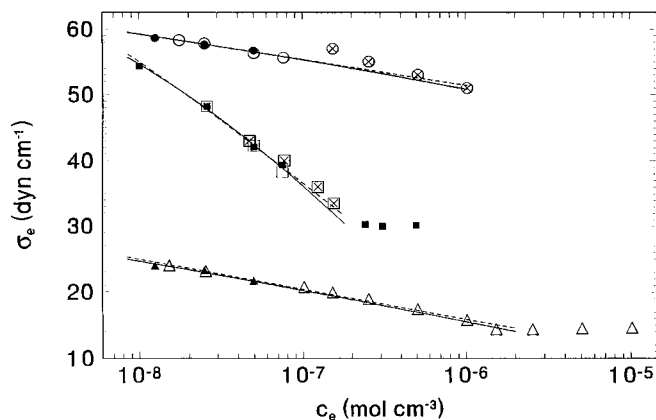
versus $t^{1/2}$ in the case of Temkin isotherm are shown in Figs. 9 and 10. Similar curves were obtained in the case of the Langmuir isotherm. Indeed, a linear relationship between Γ and $t^{1/2}$ exists at short periods of time. The initial adsorption $\Gamma(0)$ is not equal to zero. This seems reasonable because a completely surfactant-free surface can hardly exist in these experiments. The $\Gamma(0)/\Gamma_e$ values were used for calculation of the diffusivity from the slopes $\partial\sigma/\partial(t^{-1/2})$ obtained at long periods of time. The results obtained at long and short periods of time by means of Eqs. [4] and [5], respectively, are summarized in Table 2, where the values obtained by using the Langmuir isotherm are given in parentheses. In general, the diffusivities of Triton X-100 obtained are reasonable and confirm the conclusion of others that the adsorption of this surfactant occurs under diffusion control (4, 6–10). The diffusivities obtained by the Temkin isotherm are more
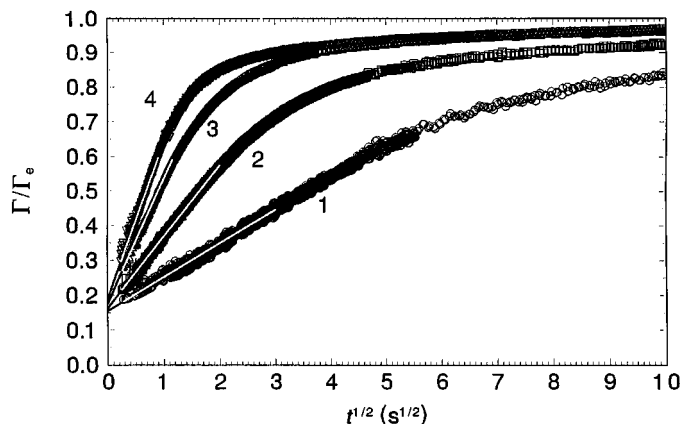

FIG. 9. Surfactant adsorption at solution/air interface calculated from the DST of Triton X-100 solutions by means of the Temkin isotherm at concentrations ($\times 10^8$ mol cm^{-3}) equal to 1.0 (1), 2.58 (2), 5.0 (3), and 7.5 (4) versus $t^{1/2}$. The lines are drawn according to Eq. [5].

FIG. 7. Dynamic surface tension of Triton X-405 solutions versus $t^{-1/2}$. Notations are the same as in Fig. 3.

TABLE 1
Parameters of the Adsorption Isotherms

System	a mol cm^{-3}	$\Gamma_\infty \times 10^{10}$ mol cm^{-2}	$\alpha \times 10^{-21}$ dyn cm^3 mol^{-2}	k_1 dyn$^{1/2}$ cm$^{-1/2}$
Triton X-100/air	1.488×10^{-9}	3.414	0.248	18.64
Triton X-405/air	5.039×10^{-12}	0.691	3.101	7.69
Triton X-405/hexane	1.975×10^{-14}	0.792	4.780	8.39

consistent and closer to the expected value of 3.5×10^{-6} cm^2/s than those obtained by the Langmuir isotherm. The diffusivities of Triton X-100 obtained by short-time approximation with the Temkin isotherm practically coincide with those obtained at long periods of time. This is not the case with Triton X-405. Its diffusivity obtained at long periods of time is more than six times lower than that at short periods of time, irrespective of the isotherm used. The average diffusivity obtained at short periods of time by the Temkin isotherm is close to the expected value 2.4×10^{-6} cm^2/s, whereas that obtained at long periods of time seems too small. Our results suggest that in contrast with Triton X-100, the adsorption of Triton X-405 is retarded at long periods of time. One can conclude that at long periods of time the adsorption of Triton X-405 is not purely diffusion controlled, but some barrier contribution exists. A similar conclusion has been reached in Ref. (5).

The above analysis needs some comments related to the applicability of Eq. [2] and to some hydrodynamic effects due to the fast method of drop formation. Indeed, switching from the dynamic (jet) regime to the static (drop) regime by closing the stopcock (Fig. 1) causes (i) a hydrodynamic shock (so-called "water hammer") due to the inertial effect and probably (ii) some turbulence inside the drop. Both effects operate for a very short period of time just after stopping the flow ($t = 0$). The shock wave causes some high-frequency pressure oscillations that damp within 30–50 ms (see Ref. (15), Fig. 2c). The turbulence may cause a vigorous agitation of the solution inside

the drop, thus equalizing the surfactant concentration just after stopping the flow and helping in better matching of the initial condition of the Ward and Tordai equation ($c_s(0) = c_e$). Some acceleration of adsorption due to agitation at very short periods of time cannot be excluded since the initial adsorption in our experiments is not found equal to zero (Table 2). However, the turbulence should disappear very fast in comparison to the evolution of the concentration profile inside the drop, because the Schmidt number ($Sc = \nu/D \sim 10^4$, where ν is the kinematic viscosity) is very large. That is why the turbulence should have a minor or no effect on the diffusion at periods of time longer than 40–50 ms after formation of the drop. The same is true for the shock wave caused by the inertial effect. Since we ignore the data collected during first 40–50 ms of the measurements (see Ref. (15)), both effects considered do not significantly affect the interpretation of the results obtained by the FFD technique.

As we have already pointed out, the Ward and Tordai equation (Eq. [2]) can be applied to curved interfaces if the depth of the diffusion layer $\delta = \Gamma_e/c_e$ is negligible in comparison to the radius of curvature R. The latter requirement is satisfied if the inequality $\delta/R < 0.1$ is fulfilled. It can be verified that this inequality is valid for all Triton X-405 solutions studied by the FFD technique ($R \geq R_c$, see Table 2). Hence, the use of Eq. [2] should not lead to any significant error in the results obtained for Triton X-405. The following values of δ/R_c are obtained:
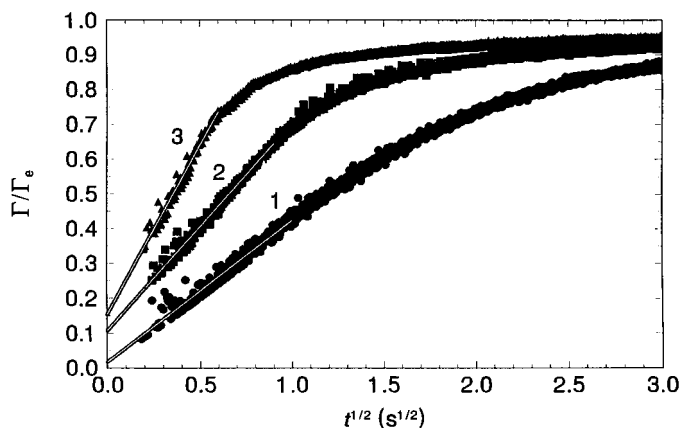

FIG. 10. The same as in Fig. 9 in the case of Triton X-405 solutions at concentrations ($\times 10^8$ mol cm^{-3}) equal to 1.25 (1), 2.5 (2) and 5.0 (3).

TABLE 2
Results Obtained from the DST and DIT at Short (Eq. [5]) and Long (Eq. [4]) Periods of Time

$c \times 10^8$ mol cm^{-3}	$\Gamma_e \times 10^{10}$ mol cm^{-2}	$\Gamma(0)/\Gamma_e$	$D \times 10^6$ (cm^2 s^{-1}) Eq. [5]	Eq. [4]
Triton X-100/air				
1.00	2.661 (2.972)^a	0.155 (0.018)	5.2 (10.3)	5.5 (11.6)
2.58	3.132 (3.228)	0.163 (0.032)	4.9 (12.1)	4.8 (7.2)
5.00	3.462 (3.315)	0.176 (0.086)	4.9 (11.4)	3.7 (3.9)
7.50	3.664 (3.348)	0.191 (0.144)	3.8 (8.0)	3.2 (2.5)
Triton X-405/air				
1.25	0.656 (0.691)	0.017 (0.000)	3.6 (11.4)	0.6 (0.8)
2.50	0.684 (0.691)	0.107 (0.155)	2.1 (8.5)	0.3 (0.3)
5.00	0.712 (0.691)	0.154 (0.401)	1.5 (3.3)	0.2 (0.1)
Triton X-405/hexane				
1.25	0.743 (0.792)	0.000 (0.000)	5.8 (24.3)	0.5 (0.6)
2.50	0.761 (0.792)	0.048 (0.165)	4.8 (24.6)	0.5 (0.5)
5.00	0.779 (0.792)	0.060 (0.280)	4.0 (13.1)	0.4 (0.2)

^{a} The values in parentheses are obtained by the Langmuir isotherm.

0.40, 0.18, 0.11, and 0.08 in the case of Triton X-100 solutions. Hence, some influence of the curvature on the results for Triton X-100 solutions at concentrations 1×10^{-8}, 2.58×10^{-8}, and 5×10^{-8} mol/cm^3 should be expected. The effect of the curvature on the adsorption in the case of an outer diffusion problem (the surfactant is outside the drop) has been studied in Ref. (6). It has been shown that the curvature effect is negligible at short periods of time ($t \ll \delta^2/D$) even at large values of δ/R. At long periods of time, however, curvature has a significant effect on dynamic adsorption. The latter is greater than the adsorption at a plane interface in the case of an outer diffusion problem. Our experiments correspond to an inner diffusion problem (the surfactant is inside the drop), and some slowing down of the adsorption process in comparison to the adsorption on a plane interface at long periods of time should be expected. Hence, the diffusivity values obtained by means of Eq. [2] at long periods of time should be smaller than those at short periods of time in the case of diluted Triton X-100 solutions. Although, this is true for some of the Triton X-100 solutions studied (see Table 2), a more profound analysis of the results suggests that the observed differences between diffusivity values at short and long periods of time are hardly due to the curvature effect. Indeed, the influence of the curvature should increase with the increase in δ/R_c. However, our results exhibit just the opposite tendency. The difference between D at short and long periods of time is largest for 5×10^{-8} mol/cm^3 Triton X-100 solution ($\delta/R_c = 0.11$), but absent for 1×10^{-8} mol/cm^3 Triton X-100 solution ($\delta/R_c = 0.4$). Comparison of the data measured by the FFD technique with those measured by the static drop weight method gives other evidence for the negligible influence of curvature on the results obtained by the former method. The radius of curvature estimated from the volume of the detached drops in static drop weight measurements is larger than 0.27 cm because a wide capillary was used in these experiments (see Ref. (15)). Hence, we obtain $\delta/R = 0.04 \ll 1$ for 2.58×10^{-8} mol/cm^3 Triton X-100 solution, while δ/R is equal to 0.18 for the same solution in the FFD measurements. Although a large difference between δ/R values exists, DST measured by both methods coincides in a whole studied time range (see Figs. 2 and 6, curve 2). One can conclude that the curvature of the interface does not significantly affect the results obtained with both surfactants in our experiments. The large differences observed between diffusivity values of Triton X-405 at short and long periods of time are not due to the curvature effect, but to some other reasons we will discuss later.

The minima of the DIT of Triton X-100 solutions observed in Fig. 4 are more easily visible in Fig. 11, where the DIT is plotted versus $t^{-1/2}$. It is seen that the slopes of the curves are negative at long periods of time, except for the first two less concentrated solutions. Minima of DIT of some nonionic surfactant solutions under similar experimental conditions have already been reported by other researchers (22, 23). They have proven, both experimentally and theoretically, that a minimum in the DIT can be observed if the following conditions are simulta-
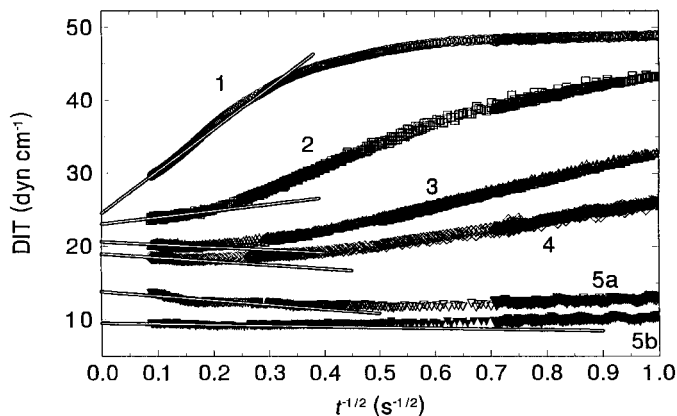

FIG. 11. Dynamic interfacial tension of Triton X-100 solutions against hexane versus $t^{-1/2}$. The experimental conditions are the same as in Fig. 4.

neously fulfilled: (i) the surfactant is soluble in both phases, (ii) the two phases are not preequilibrated with respect to the surfactant, and (iii) the volume of the surfactant-free phase is much greater than the volume of the phase containing surfactant. The same authors have determined the partition coefficients k_p of Triton X-100 and Triton X-405 in a water/hexane system (24). They found $k_p = 0.82$ for Triton X-100 and $k_p < 0.1$ for Triton X-405. The volume of the hexane phase is about 35,000 times greater than the volume of the solution (the drop phase) in our experiments. Hence, the above conditions are fulfilled in the case of Triton X-100, and minima of the DIT are observed. The absence of such minima in solutions of low concentration is probably due to the restricted duration of measurements. Indeed, the minimum of the DIT should appear later at a lower surfactant concentration (23). Our results with Triton X-100 can be qualitatively explained in the same way as done in Ref. (22). The surface mass balance equation of the present system with a mass transfer is

$$\frac{d\Gamma}{dt} = j_w - j_h,$$

where j_w and j_h are the surfactant fluxes in the water and hexane phase, respectively. Roughly, $j_w \sim (c_{ew} - c_{sw})$ and $j_h \sim (c_{eh} - c_{sh}) \approx c_{sh}$, because $c_{eh} \ll c_{sh}$ (subscripts "w" and "h" denote the water and hexane phases, respectively). In the beginning (at short periods of time), subsurface concentrations in both phases, c_{sw} and c_{sh}, are very small, and j_w is greater than j_h; hence $d\Gamma/dt > 0$. The adsorption Γ increases (DIT decreases) with time. This leads to an increase in j_h due to an increase in c_{sh} and to a decrease in j_w because c_{ew} decreases from exhaustion of the surfactant in the drop phase. At a certain moment, j_w becomes equal to j_h, and Γ reaches a maximum (the DIT is a minimum). After that, j_h prevails over j_w, and the adsorption decreases (the DIT increases). The quantitative interpretation of the results involves numerical computations and could be done similarly to Ref. (23).

We already pointed out in the previous section that neither minima nor a significant effect of preequilibration of the phases is observed in the Triton X-405/hexane system (see Fig. 5). These results suggest that the partition coefficient of Triton X-405 is not large enough to affect significantly the DIT of the solutions studied. Neglecting the possible small solubility of Triton X-405 in hexane, we have processed the DIT data in the same way as in the case of a solution/air interface. The DIT versus $t^{-1/2}$ is plotted in Fig. 12. The extrapolated DIT values at infinite time are compared with the equilibrium data obtained by van Hunsel (4) in Fig. 8. Since perfect agreement exists between both sets of data, we have fitted the data all together by Eqs. [11] or [14]. The parameters obtained are shown in the last row of Table 1. We used them for further calculations. The results obtained by means of Eqs. [4] and [5] (i.e., the short and long time approximations, respectively) are summarized in Table 2. The same discrepancy between the values of D at short and long periods of time is observed as in the case of the solution/air interface.

Our results suggest that a difference exists between the adsorption kinetics of Triton X-100 and that of Triton X-405. The adsorption of Triton X-100 occurs under diffusion control within the whole time range studied. However, the adsorption of Triton X-405 occurs under diffusion control at short periods of time, whereas some adsorption barrier seems to appear at long periods of time, thus decreasing the net rate of adsorption. The latter phenomenon is observed at both the solution/air and the solution/hexane interfaces. Since both surfactants have the same hydrophobic tail, the explanation of the observed difference is probably hidden in the difference between their hydrophilic heads. Indeed, the hydrophilic head of Triton X-405 consists of 40 EO units. Hence it is much greater than the head of Triton X-100 (10 EO units). There is evidence that the polyoxyethylene chains of surfactants with large number of EO units exist as random coils in the bulk of solution as in the adsorption layer (25–28). The size of the coils increases with an increasing num-
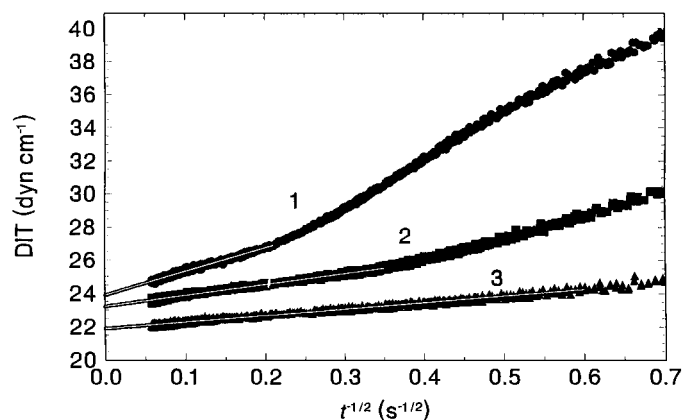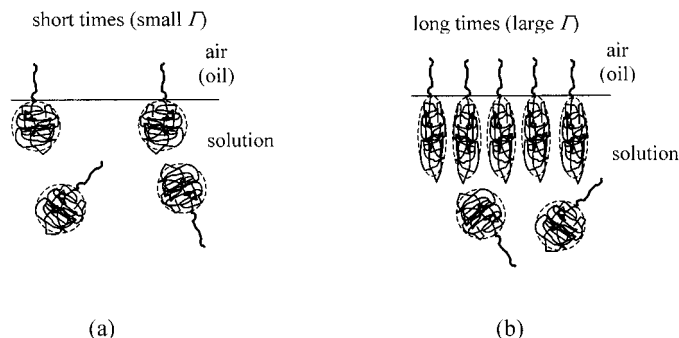

FIG. 13. Shape of the hydrophilic polyoxyethylene heads of the surfactants at short (a) and long (b) times (see the text).

ber of EO units (27, 28). Based on the above, we can draw the following hypothesis. At short periods of time, Triton X-405 molecules adsorb at the interface in the form they have in the bulk (i.e., a small hydrophobic tail connected to a large ball-like hydrophilic coil) because there is enough empty space at the interface (Fig. 13a). That is why the rate of adsorption depends mainly on the diffusion of the molecules from the bulk to the subsurface. The adsorption layer becomes more dense at long periods of time. Then there is not enough space for the adsorption of surfactant molecules with large ball-like heads. Further adsorption is possible only after some rearrangement of the EO units in the heads. Thus their shape changes to an ellipsoid elongated normal to the interface direction (Fig. 13b). The energy needed for such a rearrangement is recovered due to transfer of the hydrophobic tail from the polar (water) to the nonpolar phase (air or oil). Since the change of the head shape needs some time, the net rate of adsorption decreases at long periods of time. Such a rearrangement of the EO units in the heads of Triton X-100 molecules is more difficult, or if it exists, the effect should be less pronounced because of the smaller number of EO groups. More studies are needed to confirm or to reject the above hypothesis.

CONCLUSIONS

The fast formed drop technique is a powerful tool for studying the adsorption kinetics of surfactants at solution/air and solution/oil interfaces in the time domain from 50 ms up to several minutes. The experimental data obtained by this technique can be easily interpreted by the Ward and Tordai model in the case of diffusion controlled adsorption.

The results obtained with Triton X-100 at the solution/air interface confirm that the adsorption of this surfactant occurs under diffusion control. The adsorption of Triton X-405 at solution/air and at solution/hexane interfaces seems to occur under diffusion control at small surface coverage (short periods of time), but under mixed (diffusion–kinetic) control at large surface coverage (long periods of time). This phenomenon is probably related to changes in the shape of the large hydrophilic heads of Triton X-405 molecules.

FIG. 12. Dynamic interfacial tension of Triton X-405 solutions against hexane versus $t^{-1/2}$ at concentrations ($\times 10^8$ mol cm^{-3}) equal to 1.25 (1), 2.5 (2), and 5.0 (3).

The DIT of Triton X-100 solutions against hexane passes through a minimum due to partial solubility of the surfactant in hexane and to the restricted volume of the drop. The surfactant transport through the interface must be accounted for in interpreting the results in this case. The DIT of Triton X-405 solutions does not exhibit any peculiarities and can be properly interpreted by assuming that the surfactant is soluble only in the water phase. These conclusions are supported by the findings of other researchers obtained with nonionic surfactants under similar experimental conditions.

The proper interpretation of the experimental data depends on the type of isotherm used. More consistent results are obtained when the Temkin isotherm is used instead of the Langmuir isotherm. The diffusivities obtained at short periods of time by means of the Langmuir isotherm are much larger than expected values, especially in the case of Triton X-405 solutions.

ACKNOWLEDGMENTS

REFERENCES

1. Schick, M. (Ed.), "Nonionic Surfactants." Dekker, New York, 1967.
2. Schönefeldt, N., "Grenzflächenaktive Athyleneoxid–Addukte." Wissenschaftliche Verlagsgesellschaft, Stuttgart, 1976.
3. Schick, M. (Ed.), "Nonionic Surfactants: Physical Chemistry." Dekker, New York and Basel, 1987.
4. van Hunsel, J., Ph.D. Thesis, Antwerp University, Antwerp, 1987.
5. van Hunsel, J., and Joos, P., *Colloid Polym. Sci.* **267,** 1026 (1989).
6. Lin, S.-Y., McKeigue, K., and Maldarelli, C., *AIChE J.* **36,** 1785 (1990).
7. Fang, J., Ph.D. Thesis, Antwerp University, Antwerp, 1993.
8. Fainerman, V. B., Makievski, A. V., and Joos, P., *Colloids Surfaces A* **90,** 213 (1994).
9. Fainerman, V. B., and Miller, R., *Colloids Surfaces A* **97,** 65 (1995).
10. Fainerman, V. B., Miller, R., and Makievski, A. V., *Langmuir* **11,** 3054 (1995).
11. Horozov, T. S., and Joos, P., *J. Colloid Interface Sci.* **137,** 334 (1995).
12. Liggieri, L., Ravera, F., and Passerone, A., *J. Colloid Interface Sci.* **169,** 226 (1995).
13. Liggieri, L., Ravera, F., and Passerone, A., *J. Colloid Interface Sci.* **169,** 238 (1995).
14. Dukhin, S. S., Kretzschmar, G., and Miller, R., "Dynamics of Adsorption at Liquid Interfaces." Elsevier, Amsterdam, 1995.
15. Horozov, T., and Arnaudov, L., *J. Colloid Interface Sci.* **219,** 99 (1999).
16. Ward, A., and Tordai, L., *J. Chem. Phys.* **14,** 453 (1946).
17. Rillaerts, E., and Joos, P., *J. Phys. Chem.* **96,** 3471 (1982).
18. Joos, P., and Bleys, G., *Colloid Polym. Sci.* **261,** 1038 (1983).
19. Makievski, A. V., Fainerman, V. B., Miller, R., Bree, M., Liggieri, L., and Ravera, F., *Colloids Surfaces A* **122,** 269 (1997).
20. Reid, R., Sherwood, T., and Prausnitz, J., "Properties of Gases and Liquids." McGraw-Hill, New York, 1977.
21. van Uffelen, M., Ph.D. Thesis, Antwerp University, Antwerp, 1996.
22. Ferrari, M., Liggieri, L., Ravera, F., Amodio, C., and Miller, R., *J. Colloid Interface Sci.* **186,** 40 (1997).
23. Liggieri, L., Ravera, F., Ferrari, M., Passerone, A., and Miller, R., *J. Colloid Interface Sci.* **186,** 46 (1997).
24. Ravera, F., Ferrari, M., Liggieri, L., Miller, R., and Passerone, A., *Langmuir* **11,** 3054 (1995).
25. Bailey, F. E., Jr., and Koleske, J. V., in "Poly(ethylene) Oxide," pp. 29–86. Academic Press, New York, 1976.
26. Guvelly, D., Davis, S., and Kayes, J., *J. Colloid Interface Sci.* **91,** 1 (1983).
27. Schick, M., *J. Colloid Sci.* **17,** 801 (1960).
28. Schick, M., *J. Am. Oil Chem. Soc.* **40,** 680 (1963).